Hybrid Logical-Physical Qubit Interaction for Quantum Metrology

Supplemental Material

Nadav Carmel* and Nadav Katz†

The Hebrew University of Jerusalem

(Dated: May 26, 2023)

CONTENTS

I. THEORETICAL BACKGROUND

A. Difference Measures between Density Matrices

We define the Distance between two quantum states ρ, σ to be

$$D(\rho, \sigma) = Tr|\rho - \sigma|^2 \tag{S1}$$

With $|A| = \sqrt{A^\dagger A}$ the positive square root of $A^\dagger A$. It is possible to prove that our definition of *Distance* behaves the same as the widely used *Trace Distance* defined as $\frac{1}{2}Tr|\rho - \sigma|$ [1].

* nadav.carmel1@huji.mail.ac.il

† nadav.katz@mail.huji.ac.il

In addition, we use the regular definition of *Fidelity*,

$$F(\rho, \sigma) = Tr\sqrt{\rho^{1/2}\sigma\rho^{1/2}} \tag{S2}$$

We can see it approaches 1 as the states are closer and approaches 0 when they are not.

B. Quantum Phase Estimation

Quantum phase estimation is a family of algorithms. Although it is a knowledge common in the community, for completeness we give here brief description of the main idea of quantum phase estimation, and two iterative implementations of it. Suppose a unitary operator U has an eigenvector $|u\rangle$ with eigenvalue $e^{2\pi i\phi}$, where the value of ϕ is unknown. The goal of the phase estimation algorithm is to estimate ϕ. To perform the estimation, we assume we have available black boxes capable of preparing the state $|u\rangle$ and performing controlled-U^{2^j} operations for some positive integer j. The algorithm uses two quantum registers, one for the measured operator U and one for ancilla qubits needed for the computation. Phase estimation was first introduced by Kitaev [2].

1. Kitaev's Iterative Phase Estimation

By introducing the m-bit approximation denoted as $\tilde{\phi} = 0.\phi_1\phi_2\ldots\phi_m$, and defining $\alpha_k = 2^{k-1}\tilde{\phi}$, the utilization of the circuit illustrated in figure 1 (a) of the main text leads to the following relations: for the application of $K = I$, we obtain $\cos(2\pi\alpha_k) = 2P(0|k) - 1$, and for the application of $K = S$, we have $\sin(2\pi\alpha_k) = 1 - 2P(0|k)$. This information is sufficient for the extraction of α_k. Upon obtaining all α_k values for k ranging from 1 to m, we can then retrieve the approximation $\tilde{\phi}$ using algorithm 1.

2. Iterative Phase Estimation Algorithm

The Iterative Phase Estimation (IPEA) method, as depicted in figure 1 (a) of the main text [3], utilizes a single ancilla qubit for performing phase estimation. This characteristic renders it particularly valuable in the context of Noisy Intermediate Scale Quantum (NISQ) computers, given the current limitations on the simultaneous utilization of multiple qubits. It is worth noting that the implementation of this circuit is challenging, and recent

research [4] has demonstrated its feasibility. Several recent studies [5–7] have highlighted the significant potential of the IPEA algorithm. A notable advantage of this algorithm is its success probability, which, in an ideal scenario, remains independent of the desired number of measured digits.

Algorithm 1: Kitaev Estimator

Result: $\tilde{\phi} = 0.\phi_1\phi_2...\phi_{m+2}$ the $(m+2)$-bit approximation to the phase ϕ

1 Estimate all α_k using the circuit in figure 1 (a) of the main text;

2 Set $\beta_m = 0.\phi_m\phi_{m+1}\phi_{m+2}$ where β_m is the closest octant $\{\frac{0}{8}, \frac{1}{8}, ..., \frac{7}{8}\}$ to α_m ;

3 **for** $j = m-1$ **to** 1 **do**

4 $$\phi_j = \begin{cases} 0 \text{ if } |0.0\phi_{j+1}\phi_{j+2} - \alpha_j|_{mod1} < 1/4 \\ 1 \text{ if } |0.1\phi_{j+1}\phi_{j+2} - \alpha_j|_{mod1} < 1/4 \end{cases}$$

5 **end**

II. THE 5-QUBIT CODE

The 5-qubit code is a stabilizer code defined by the stabilizers in table S1 or by the logical basis states defined in equations S3, S4. As mentioned in the main text, any error in one or two qubits will result in measuring a non trivial syndrome. This phenomena of the 5-qubit code is represented in table S2. It's basis states are the following:

$$\begin{aligned} |1\rangle_L = \frac{1}{4}\big[&|11111\rangle + |01101\rangle + |10110\rangle + 01011\rangle \\ &+|10101\rangle - |00100\rangle - |11001\rangle - 00111\rangle \\ &-|00010\rangle - |11100\rangle - |00001\rangle - |10000\rangle \\ &-|01110\rangle - |10011\rangle - |01000\rangle + |11010\rangle\big] \end{aligned} \tag{S3}$$

$$\begin{aligned} |0\rangle_L = \frac{1}{4}\big[&|00000\rangle + |10010\rangle + |01001\rangle + 10100\rangle \\ &+|01010\rangle - |11011\rangle - |00110\rangle - 11000\rangle \\ &-|11101\rangle - |00011\rangle - |11110\rangle - |01111\rangle \\ &-|10001\rangle - |01100\rangle - |10111\rangle + |00101\rangle\big] \end{aligned} \tag{S4}$$

All necessary logical gates that were not defined in the main text are depicted in figure S1.

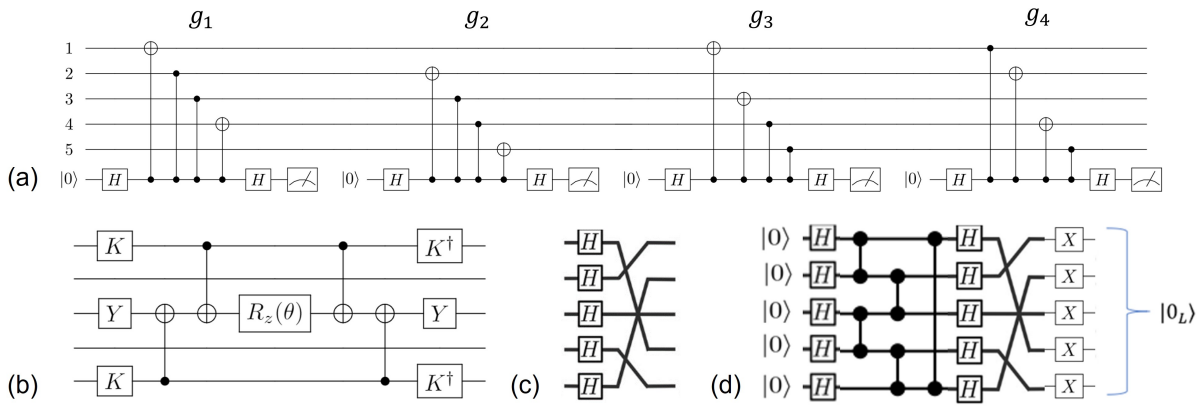

FIG. S1: (a) Logical Post Selection is essentially applying syndrome extraction and post selecting the results that are in the code (trivial syndrome). (b) The logical $R_z(\theta)$ by [8]. (c) The logical Hadamard gate by [8]. (d) State preparation for the 5-qubit code, inspired by [9].

Generator Table for the 5-Qubit Code	
g_1	$X_1Z_2Z_3X_4$
g_2	$X_2Z_3Z_4X_5$
g_3	$X_1X_3Z_4Z_5$
g_4	$Z_1X_2X_4Z_5$

TABLE S1: Generator Table for the 5-Qubit Code

III. SCALING OF THE ERROR PROBABILITY

In this section we dive deeper into understanding the notion of logical post selection, and analyse the new scaling of the error probability. The incentive of developing a deeper understanding appears in table S2, where we can see that errors in two or less qubits will result in measuring the trivial syndrome. In our error analysis we follow the explanation by Neilsen and Choung [1].

Here, we present a simple error analysis of LPS for the five qubit code. We assume the depolarising channel with probability p acts on the state, giving

$$\rho \to (1-p)\rho + \frac{p}{3}(X\rho X + Y\rho Y + Z\rho Z) \tag{S5}$$

For a simple one physical qubit case, taking a pure state $\rho = |\psi\rangle\langle\psi|$, we get process fidelity

Error Syndrome $\langle g_1, g_2, g_3, g_4 \rangle$	Possible Cause
0000	IIIII
0001	XIIII, IIYYI, IIZIX, IXIZI, IYXII, IZIIZ, IIIXY
0010	IIIIX, IIXYI, IYYII, IZIXI, XIZII, YXIII, ZIIZI
0011	IIZII, IIIXZ, IYIYI, IZIIY, XIIIX, YIIZI, ZXIII
0100	IIIXI, IIZIZ, IXYII, IZIIX, XIIIY, YYIII, ZIXII
0101	IIIIY, IIYZI, IXIYI, IZZII, XIIXI, YIXII, ZYIII
0110	IZIII, IIIXX, IIXZI, IIZIY, XIIIZ, YIYII, ZIIYI
0111	IIIIZ, IIZXI, IXXII, IYIZI, XZIII, YIIYI, ZIYII
1000	IIXII, IIIYX, IXIIZ, IZIZI, XYIII, YIIIY, ZIIXI
1001	IYIII, IIIZZ, IIYIX, IIZYI, XIXII, YIIXI, ZIIIY
1010	IIIYI, IIXIX, IXIIY, IYZII, XIYII, YIIIZ, ZZIII
1011	IIYII, IIIZY, IXIXI, IYIIX, XIIYI, YZIII, ZIIIZ
1100	ZIIII, IIIZX, IIXXI, IIYIZ, IXZII, IYIIY, IZIYI
1101	YIIII, IIIYZ, IIXIY, IIZZI, IXIIX, IYIXI, IZYII
1110	IIIZI, IIYIY, IYIIZ, IZXII, XXIII, YIZII, ZIIIX
1111	IXIII, IIIYY, IIXIZ, IIYXI, XIIZI, YIIIX, ZIZII

TABLE S2: Error syndrome and possible cause for the 5 qubit code. Causes with errors in more then 2 qubits are neglected.

of

$$\begin{aligned} F &= \sqrt{\langle\psi|\rho|\psi\rangle} \\ &= \sqrt{(1-p) + \frac{p}{3}[\langle\psi|X|\psi\rangle^2 + \langle\psi|Y|\psi\rangle^2 + \langle\psi|Z|\psi\rangle^2]} \end{aligned}$$

This expression gets the lowest fidelity for $|\psi\rangle = |0\rangle$, with:

$$F = \sqrt{1 - \frac{2}{3}p} = 1 - \frac{p}{3} + O(p^2)$$

Now, for the logical qubit. Assume we encode one qubit of information into n physical qubits, each goes through a depolarizing channel ε with probability p, as in equation S5.

Then the channel's action on a state ρ becomes:

$$\varepsilon^{\otimes n}(\rho) = (1-p)^n\rho + \sum_{j=1}^{n}\sum_{k=1}^{3}(1-p)^{n-1}\frac{p}{3}\sigma_k^j\rho\sigma_k^j$$

$$+\sum_{j_1=1}^{n}\sum_{j_2=1}^{n}\sum_{k_1=1}^{3}\sum_{k_2=1}^{3}(1-p)^{n-2}\frac{p^2}{9}\sigma_{k_1}^{j_1}\sigma_{k_2}^{j_2}\rho\sigma_{k_2}^{j_2}\sigma_{k_1}^{j_1} + ...$$

With σ_k^j being the k'th Pauli operator acting on the j'th qubit. The first element represents one faulty qubit and the second represents two faulty qubits, and the dots represent errors in more then 2 qubits, which are neglected. Now, after performing LPS, each element in this sum will be returned to the state ρ given ρ was in the code:

$$(R\otimes\varepsilon^{\otimes n})(\rho) = \left[(1-p)^n\rho + np(1-p)^{n-1} + \binom{n}{2}p^2(1-p)^{n-2}\right]\rho$$

And finally, the fidelity F remains:

$$\begin{aligned} F &\geq \sqrt{(1-p)^{n-2}(1+(n-2)p+(\frac{n(n-1)}{2}-n+1)p^2)} \\ &= 1-\frac{1}{12}n(n^2-3n+2)p^3+O(p^4) \end{aligned} \tag{S6}$$

Giving a p^3 dependence and confirming our intuition from table S2.

Kitaev's phase estimation circuit, when applied with $K = I$, demonstrates a high level of fault-tolerance, with the exception of the state preparation and the hybrid entangling operation stages, which are not fault-tolerant. Consequently, this circuit can be employed to approximate the scaling of the error probability after logical post-selection. The logical post-selection occurs after the entire iteration, necessitating the consideration of the error probability as the likelihood of a single error occurring in a single qubit throughout the entire iteration. Since the circuit exhibits transversality in most of it's stages, such an error approximately does not propagate to other qubits. The error probability can be derived using the equation:

$$P_{error} = 1 - F^2 \tag{S7}$$

Here, F represents the fidelity calculated according to equation S2 from figure 2 (c) of the main text. The analysis illustrated in figure S2 confirms that the best approximation to the scaling is not a second or fourth degree polynomial, but rather a third degree polynomial, as anticipated based on our theoretical derivations.

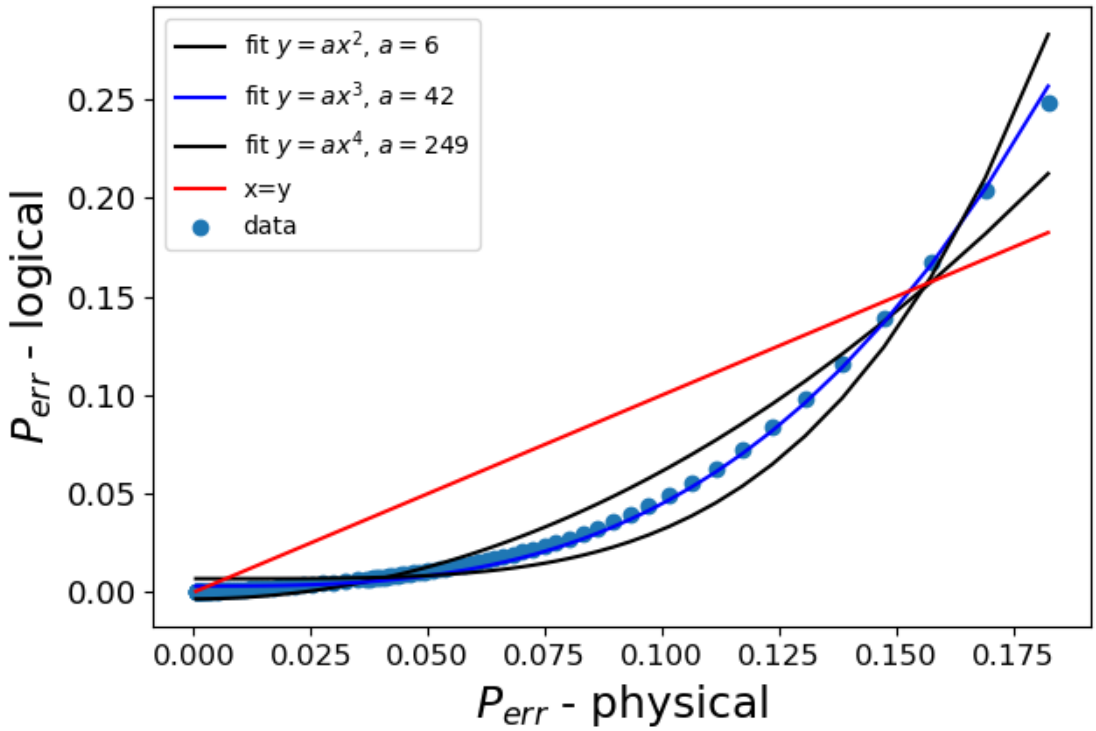

FIG. S2: Confirming the error probability as predicted by equation S6. Error probability extracted from fidelity according to equation S7.

IV. ADDITIONAL RESULTS - KITAEV QPE

In this section we develope an understanding to the use of accelerated hamiltonians in the resource-limited case. Here the settings are the same as in figure 2 (c) of the main text, i.e: perfect sensor and noisy ancilla. The relevant sizes for the problem are the ideal probability for the ideal circuit without noise P_i, the ideal probability for the noisy circuit P_n and the estimate to that probability $\tilde{P}_n$ obtained by $m = N(1-li)$ successful trials, with li being the same lost information as in the main text. We define the distance between the ideal circuit's probability and the noisy circuit's ideal probability by $|d| = |P_n - P_i| = D/\sqrt{2}$, Where D is given in equation S1. Following reference [10] we demand that the error in estimating the ideal probability be confined, such that the probability that the algorithm succeeds is (by the addition rule for statistical and systematic errors)

$$Pr\left(\sqrt{|\tilde{P}_n - P_n|^2 + \frac{D^2}{2}} < \frac{2-\sqrt{2}}{4}\right)$$

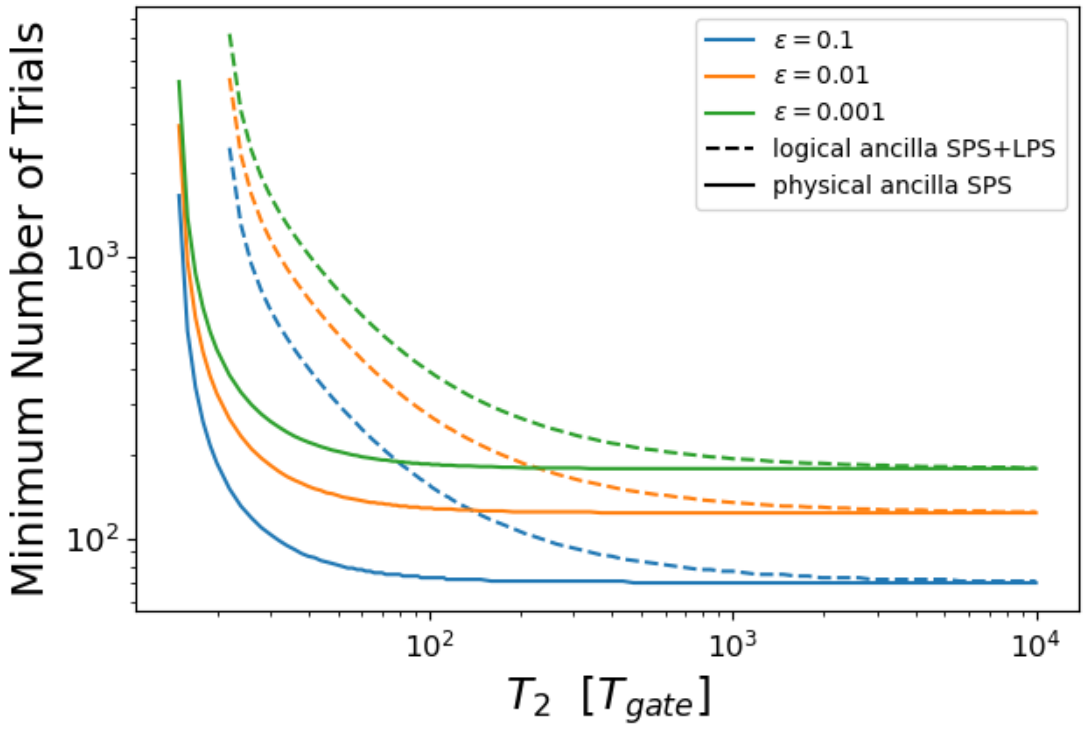

FIG. S3: Minimal number of trials for Kitaev's algorithm to succeed according to Eq. S9, obtained by the data of figure 2 (c) of the main text.

This equals to

$$Pr\left(|\tilde{P}_n - P_n|^2 < \left(\frac{2-\sqrt{2}}{4}\right)^2 - \frac{D^2}{2}\right)$$

So, the first conclusion is that the algorithm fails for T_2 such that

$$D(T_2) > \frac{\sqrt{2}-1}{2} \tag{S8}$$

We conclude that the probability for the algorithm to fail (by applying Chernoff bound) is

$$Pr\left(|\tilde{P}_n - P_n| \geq \sqrt{\left(\frac{2-\sqrt{2}}{4}\right)^2 - \frac{D^2}{2}}\right) \leq$$
$$2e^{-2((\frac{2-\sqrt{2}}{4})^2 - \frac{D^2}{2})m}$$

and we demand that the probability to succeed is

$$Pr\left(|\tilde{P}_n - P_n| < \sqrt{\left(\frac{2-\sqrt{2}}{4}\right)^2 - \frac{D^2}{2}}\right) \geq 1-\epsilon$$

This gives us a Minimum of

$$N > \frac{\ln(\frac{2}{\epsilon})}{2(1-li(T_2))((\frac{2-\sqrt{2}}{4})^2 - \frac{(D(T_2))^2}{2})} \tag{S9}$$

trials for the algorithm to succeed with probability of success $p \geq 1-\epsilon$. Calculating this value for noise of different strengths and for a number of different ϵ's we get the expected result of Fig. S3, showing no improvement of the logical approach over the physical one.

V. ADDITIONAL RESULTS - IPEA

A. Sensing

Here we present the two additional scenarios complementing the one in the main text: a scenario where the sensor is put in the excited state and is susceptible to T_1 noise, with perfect ancillas, measuring $R_z(\frac{2\pi}{\sqrt{3}})$ (Fig. S4 (a)), and a scenario in which we measure $R_z(\frac{2\pi}{\sqrt{3}})$ with sensor qubit initialized in the excited state $|1\rangle$, with noisy (dephasing) ancillas and perfect sensor (Fig. S4 (b)) - this is the sanity check.

B. Computing

First we present some additional results on the structure of the histogram of possible results to complete the picture provided by Fig.2d, Fig3 in the main text. In figure S4 (c) is Fig.3b of the main text in a logarithmic scale, and S4 (d) presents the bare standard deviation of the histogram.

In some cases we are instead interested in applying the algorithm only once and assess it's probability to give the right result. In such cases, where the sensing or computation time has a lower importance, it is convenient to have an oracle stating whether the result is reliable or not. Implementation of IPEA is possible both in two types of systems:

1. Ensemble systems, where it is convenient to apply the whole algorithm in parallel on a large number of qubits and measure result statistics.

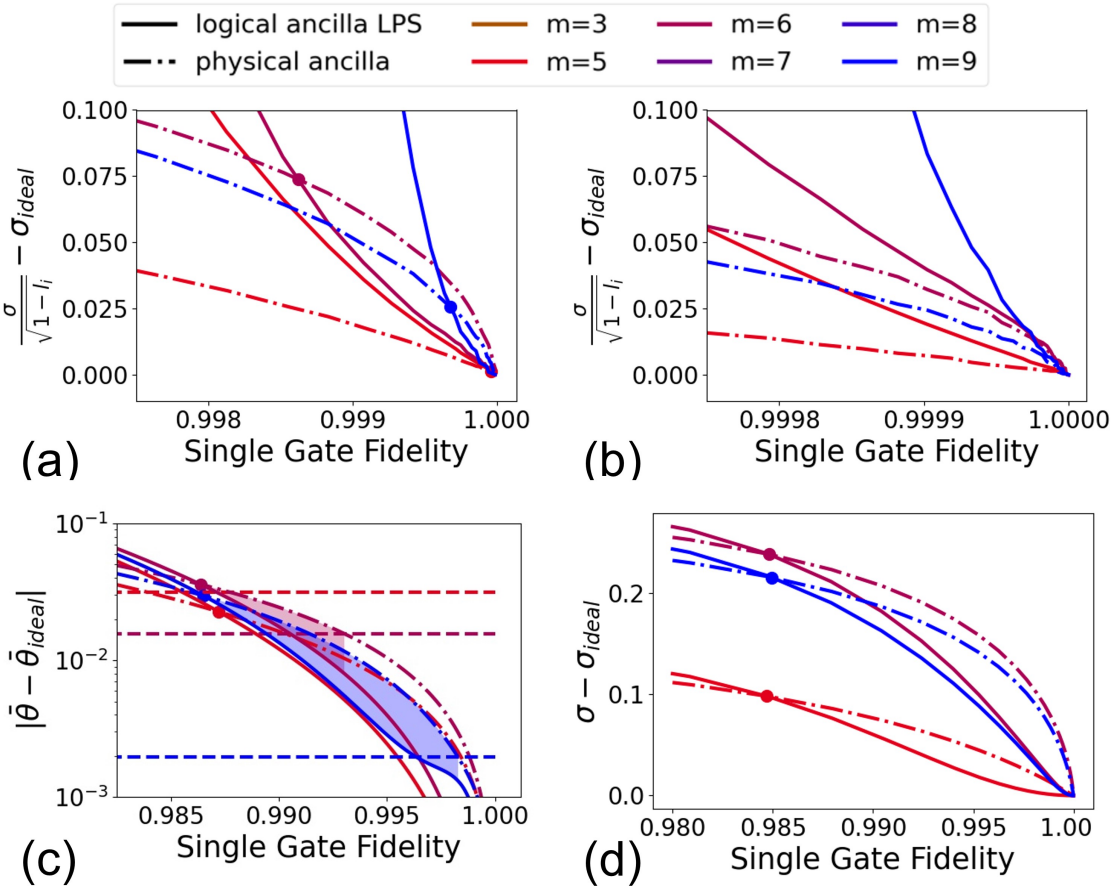

FIG. S4: Additional results for the histogram of possible results of IPEA in the presence of noise. (a-b) Error in estimating the phase of non-accelerated signal Hamiltonian $R_z(\theta)$ with sensor initialized in the state $|1\rangle$, in comparison to the ideal, using IPEA. The relative error is plotted for desired precision of 5,6,9 digits, while continuous line represents physical ancilla and dashed line represents logical ancilla and LPS. The scenario is *Resource: Minimal Number of Trials*. (a) The ancillas are perfect and the sensor is noisy, susceptible only to amplitude damping. The relevant thresholds are the crossings of dashed and continuous lines of the same color. (b) The ancillas are noisy, susceptible only to dephasing, and the sensor is perfect. It is clear that with non-accelerated Hamiltonian and perfect sensor, adding noisy ancillas does not improve sensing capabilities with IPEA. (c) Fig.3b from the paper, in a logarithmic scale. (d) Base standard deviation of the histogram. It is apparent that the thresholds in those cases, which does not take lost information into account, are around 0.985 single qubit gate fidelity.

2. Superconducting systems, where it is convenient to measure the digit in each iteration a number of times and take a majority vote.

Here we first explain how to calculate an upper bound to the error probability of the ensemble scenario, and then we show our simulated error probability for the superconducting scenario. In both cases the success probability is defined to be:

$$P_{success} = \sum_{\phi \in [\tilde{\theta}, \tilde{\theta}+2^{-m}]} p(\phi) \tag{S10}$$

Where θ is the measured phase, $\tilde{\theta}$ is the best $m-$bit approximation to it from below, and ϕ is a possible result of the algorithm. $p(\phi)$ is the probability to measure ϕ and $P_{error} = 1 - P_{success}$.

Assume an experiment contains n runs of the whole algorithm, and the result is taken to be a majority vote on the most probable interval. Then

$$\begin{aligned} P_{error} &\leq P(\text{less then } n/2 \text{ trials in the interval}) \\ &= P(0 \text{ successes in } n \text{ trials}) + P(1 \text{ successes in } n \text{ trials}) + P(\lfloor n/2 \rfloor \text{ successes in } n \text{ trials}) \end{aligned}$$

Each of the probabilities in the above formula is distributed binomialy, and so it is possible to exactly compute P_{error} [11].

Now assume the experiment contains n runs for each bit and the result for the bit is taken to be a majority vote. This has the largest impact only on the first (least significant) digits. There are only two possible results - 0 is measured or 1 is measured. Thus the probaility to measure 0 is updated in our simultaion to be the probability to measure 1 less then half of the times, and vice versa:

$$p(0) \leftarrow \sum_{k=0}^{\lfloor n/2 \rfloor} \binom{n}{k} p_1^k p_0^{n-k} \qquad\qquad p(1) \leftarrow \sum_{k=0}^{\lfloor n/2 \rfloor} \binom{n}{k} p_0^k p_1^{n-k} \tag{S11}$$

And the error probability is defined as in Eq.S10.

VI. SIMULATION DETAILS

A detailed description of the simulation and a code guide are available in the following GitHub repository. Here we give only a brief description of the simulation.

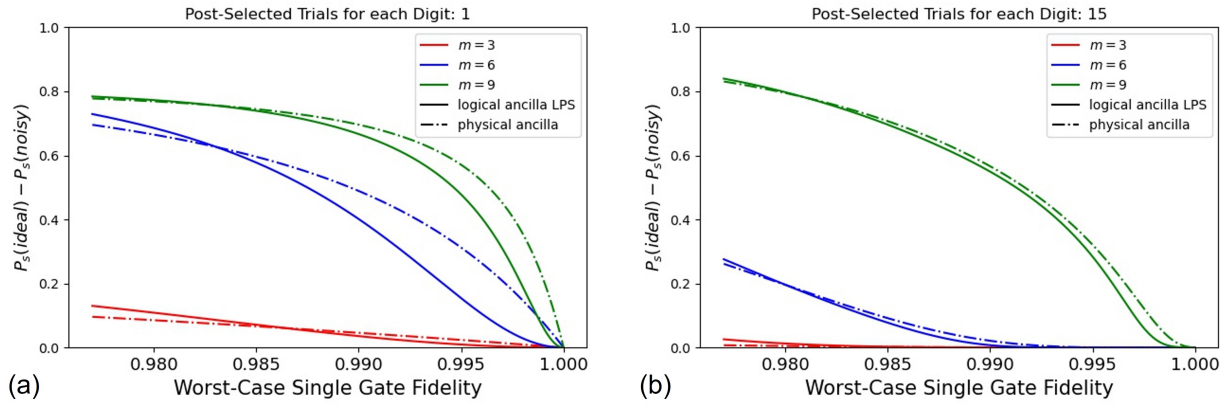

FIG. S5: Scaling of the Success probability as a function of noise for different n's. The histogram is calculated by Eq.S11 and the success probability is calculated by S10 under the assumption that the interval contains only two bins. It is apparent that increasing n leads to some flattening of the probability difference and to a larger proximity of the physical and logical control methods.

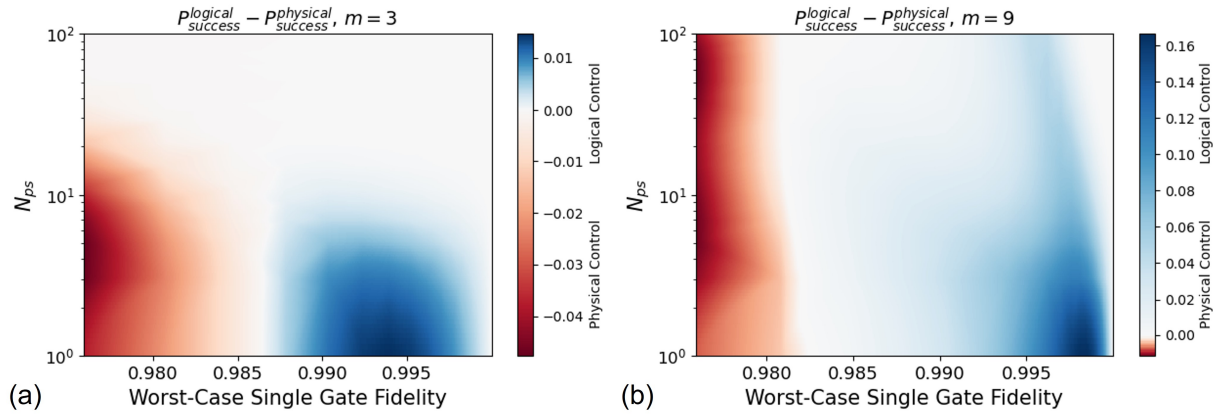

FIG. S6: A two dimensional map of the success probability difference between physical and logical control methods for different desired precision of $m = 3$ and $m = 9$ digits. the X-axis is the worst case single qubit gate fidelity and the Y-axis is the number of post selected trials for each digit. It is apparent that from a circuit depth of around a few dozens of gates, there is a threshold in approximately 0.98-0.985 worst case gate fidelity. These results are well within the capabilities of today's hardware.

A. GitHub Code

All relevant code is open for use in this GitHub repository or in the following url: `https://github.com/nadavcarmel40/paper_recalc`. To install and use the package, just install QuTiP (`https://qutip.org/docs/latest/installation.html`) by following the instructions on the above web page. The basic tool enabling the simulations can be found under the 'simulators' folder in the attached GitHub repository. 'BigStepSimulator' is a state-vector simulator and 'SmallStepSimulator' is a density matrix simulator. The state vector simulator is fast and can simulate quantum circuits without noise, and the density matrix simulator is slower and can simulate noisy circuits.

B. General Description

In this Work, we use a full density matrix simulation, similar to Ref.[12]. We save the quantum state of n qubit register as a 2-d matrix of dimensions $[2^n, 2^n]$. Operators are saved as a $[2^n, 2^n]$ matrix, and if the quantum state was initially ρ then performing the operation U on the density matrix is equivalent to updating the density matrix $\rho \to U\rho U^\dagger$.

The noise in the simulation is based on Krauss operators (more of them in appendix I). The simulation is thus made up of many small time steps, with repeated application of Krauss based decoherence in one small time-step and gate-based evolution in the next small time-step. A description of the simulation is given in figure S7 along with algorithm 2.

Defining the Pauli operator σ_i^q acting on qubit q as a tensor product of σ_i in the q index and Identity operators in all other indexes, we take the base Hamiltonian $H_0 = \bigotimes_{q=1}^{N} \frac{\hbar\omega_{01}}{2}\sigma_z^q$ to represent the free evolution of the quantum register, with $\omega_{01} = 6[GHZ]$. Practically $\hbar$ is so small that the computer takes the time evolution operator to be the identity, but defining different, large enough ω_{01} for each qubit will result in the mentioned base Hamiltonian.

In each gate-step, possibly many gates act upon the register. Thus, we start with the base Hamiltonian $H = H_0$ and for each gate G in the gate-step we find it's corresponding Hamiltonian H_G given by $G = e^{iH_G}$ and update the Hamiltonian to be $H \to H + H_G$. Now, we define the evolution operator U to be $e^{iH\frac{dt}{T_g}}$, and we apply this evolution as in step 4 of algorithm 2 for a total of T_g/dt times with decoherence step between each application of U.

The main parameters used in each simulation are the number of qubits N, the time

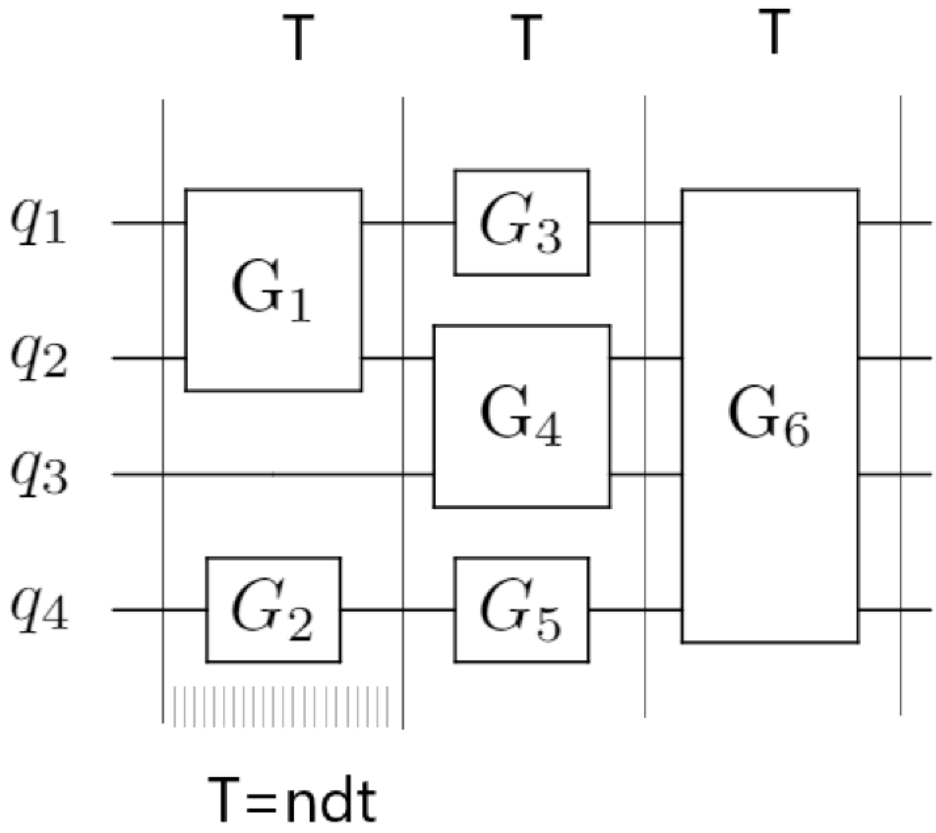

FIG. S7: Simulation of a general circuit. Each gate-step T has length T_g and is made up of $n = 20$ small time-steps of size T_g/n.

Algorithm 2: Noisy Circuit Simulation

Result: Density matrix of the register after a noisy quantum circuit.

for *gate-step* T **do**
  $U_{dt}^T = e^{i\frac{dt}{T}\sum_i H_i}$;
  for t **do**
    $\rho_{t+1} = U_{dt}^T \rho_t (U_{dt}^T)^\dagger$;
    for *qubit* **do**
      amplitude damping ;
      dephasing ;
    end
  end
end

$T_g = n \cdot dt$ $(n = 20)$ of each gate-step, the dephasing time of qubit q, T_2^q and the energy relaxation time T_1^q of the same qubit. From these parameters we define the error rates for each process and qubit:

$$p^q_{decay} = 1 - e^{-\frac{dt}{T_1^q}}$$

and

$$p^q_{dephase} = 1 - e^{-\frac{dt}{T_2^q}}$$

The decoherence is then enacted upon the register through a for-loop on each qubit, updating the register state to be:

$$\rho = E_1^q \rho (E_1^q)^\dagger + E_2^q \rho (E_2^q)^\dagger$$
$$\rho = \left(1 - \frac{P^q_{dephase}}{2}\right)\rho + \frac{P^q_{dephase}}{2}\sigma_Z^q \rho \sigma_Z^q$$

where the first equation uses the Pauli-matrix representation of the Krauss operators: $E_1^q = \frac{\sqrt{1-P^q_{decay}}}{2}(I - \sigma_Z^q) + \frac{1}{2}(I + \sigma_Z^q)$ and $E_2^q = \frac{\sqrt{P^q_{decay}}}{2}(\sigma_X^q + i\sigma_Y^q)$, and the second equation is a result of applying the phase damping channel's Krauss operators $\sum_i K_i \rho K_i^\dagger$ with probability $P^q_{dephase}$. These Krauss operators are given in the literature in their matrix form [1].

C. Measurement and Lost Information

There are two kinds of measurements we perform - post selection measurements and probabilistic measurements. Here, we first refer to the post selection measurements. Post selection measurements are done on the sensor qubit for SPS, on flag qubits for fault-tolerance, and on an additional ancilla qubit for LPS. To perform post selection measurements, we collapse the register state as defined below according to the preferred measurement outcomes. One could say we choose the system's trajectory. First, to add qubits to the simulation, we expand the register state with a tensor product to the additional qubit sub-spaces. Next, we perform the entangling operations with the additional qubits, and finally project on the trivial flag state $|0..0\rangle$ using the operator defined below. For probabilistic measurements (e.g. Error correction measurements), to decide measurement outcome on the qubit group $A = \{q_{k_1}, ..., q_{k_n}\}$, remaining with $B = \{q_1, ..., q_N\}/A$, we trace out B to get $\rho^A = Tr_B(\rho)$. Then, we define P as the diagonal of ρ^A and P' as the cumulative sum of P. we take a random number $0 < x < 1$ and find the first index i such that $x < P'[i]$. The result of the

measurement is the binary string of $i-1$. To collapse the quantum state to a state after measuring qubits in the group A, we use the following projector:

$$P_m = \bigotimes_{q=1}^{N} \begin{cases} I_2 & \text{if } q \notin A \\ \frac{I+\sigma_Z^q}{2} & \text{if } q \in A \text{ and measurement result is } |0\rangle \\ \frac{I-\sigma_Z^q}{2} & \text{if } q \in A \text{ and measurement result is } |1\rangle \end{cases}$$

And after this projection operation $\rho \to P_m \rho P_m^\dagger$ we trace out the additional qubits. The procedure described above can cause numeric errors when the state decoheres for a long time, because the projection operation as described is not trace preserving. To have a valid density matrix, for each projection, say the k'th projection, we first save the state's trace as Ps_k and then normalize the state. To calculate the portion of information that have been lost due to post selection, we use the following reasoning:

- After one projection, we have lost $1 - Ps_1$ information and remain with a state with trace Ps_1.
- After the second projection, we have lost $Ps_1 \cdot (1 - Ps_2)$ more information.
- After the third projection, we have lost $Ps_1 \cdot Ps_2 \cdot (1 - Ps_3)$ more information.
- After the k'th projection, we have lost $Ps_1 \cdot ... \cdot Ps_{k-1} \cdot (1 - Ps_k)$ more information.

Overall, this is the amount of *lost information*:

$$l_i = \sum_i ((\prod_k^{i-1} Ps_k) \cdot (1 - Ps_i)) \tag{S12}$$

---

[1] M. A. Nielsen and I. L. Chuang, *Quantum computation and quantum information* (Cambridge University Press, 2010) p. 676.

[2] A. Y. Kitaev, Quantum measurements and the Abelian Stabilizer Problem, , 1 (1995), arXiv:9511026 [quant-ph].

[3] M. Dobšíček, G. Johansson, V. Shumeiko, and G. Wendin, Arbitrary accuracy iterative quantum phase estimation algorithm using a single ancillary qubit: A two-qubit benchmark, Physical Review A - Atomic, Molecular, and Optical Physics **76**, 10.1103/PhysRevA.76.030306 (2007).

[4] M. Takita, K. Inoue, S. Lekuch, Z. K. Minev, J. M. Chow, and J. M. Gambetta, Exploiting dynamic quantum circuits in a quantum algorithm with superconducting qubits, (2021), arXiv:arXiv:2102.01682v1.

[5] S. Kais, A Universal Quantum Circuit Scheme For Finding Complex Eigenvalues, arXiv:arXiv:1302.0579v5.

[6] S. Johnstun and J.-F. Van Huele, Optimizing the Phase Estimation Algorithm Applied to the Quantum Simulation of Heisenberg-Type Hamiltonians, (2021), arXiv:2105.05018.

[7] P. M. Q. Cruz, G. Catarina, and R. Gautier, Optimizing quantum phase estimation for the simulation of Hamiltonian eigenstates, , 1 (2020), arXiv:arXiv:1910.06265v2.

[8] T. J. Yoder, R. Takagi, and I. L. Chuang, Universal fault-tolerant gates on concatenated stabilizer codes, Physical Review X **6**, 10.1103/PhysRevX.6.031039 (2016), arXiv:1603.03948.

[9] R. Chao and B. W. Reichardt, Fault-tolerant quantum computation with few qubits 10.1038/s41534-018-0085-z (2017), arXiv:1705.05365.

[10] H. Ahmadi and C.-F. Chiang, Quantum Phase Estimation with Arbitrary Constant-precision Phase Shift Operators, (2010), arXiv:1012.4727.

[11] K. Butler and M. Stephens, The Distribution of a Sum of Binomial Random Variables, (2016).

[12] S. Cheng, C. Cao, C. Zhang, Y. Liu, S.-Y. Hou, P. Xu, and B. Zeng, Simulating Noisy Quantum Circuits with Matrix Product Density Operators 10.1103/PhysRevResearch.3.023005 (2020), arXiv:2004.02388.